BENCHMARK DATABASE ON THE EVOLUTION OF TWO-PHASE FLOWS IN A VERTICAL PIPE

D. Lucas, M. Beyer, J. Kussin, P. Schütz

Forschungszentrum Dresden-Rossendorf e.V., Institute of Safety Research
P.O.Box 510 119, 01314 Dresden, Germany
Phone: +49 (0) 351 260 2047, Fax: +49 (0) 351 260 12047
D.Lucas@fzd.de

Abstract
Basing on many years of experience a new extensive high quality database was obtained for stationary upward air-water flows in a vertical pipe with an inner diameter of 195.3 mm using the wire-mesh sensor technology. During the experiments the sensor was always mounted on the top of the test section while the distance between gas injection and measuring plane was varied to up to 18 different L/D by using gas injection chambers at different vertical positions. The gas was injected via holes in the pipe wall. In this new test series the pressure was kept at 0.25 MPa (absolute) at the location of the active gas injection while the temperature was constant at 30°C ± 1K. The experiments were done for 48 combinations of air and water superficial velocities varying from 0.04 m/s to 1.6 m/s for water and 0.0025 m/s to 3.2 m/s for air. From the raw data time averaged data as: radial gas volume fraction profiles, bubble size distributions, radial volume fraction profiles decomposed according to the bubble size and the radial profiles of the gas velocity were calculated. All data were checked regarding their consistency. They are characterized by a high resolution in space what makes them suitable for the development and validation of CFD-grade closure models, e.g. for bubble forces and coalescence and break-up. It is also an ideal base to validate CFD approaches for poly-dispersed flow. For this reason it is proposed to use the database as a benchmark for modelling poly-dispersed flows.

1. INTRODUCTION

The use of Computational Fluid Dynamics (CFD) codes for simulations of two-phase flow phenomena related to Nuclear Reactor Safety research requires the qualification of the basic model concepts as well as closure models. The qualification procedure includes model development, test and validation. Especially in case of poly-dispersed flows there are still many open questions which have to be answered. Thus e.g. the presently available models for bubble coalescence and break-up are weak and can predict the evolution of the flow only for a narrow range of flow conditions. Experimental data with high resolution in space and time are required for the model improvement.

The aim of the experiments presented in this paper is to provide a high-quality CFD-grade database for upwards air/water flows in a vertical pipe with a nominal diameter of 200 mm. This includes different flow pattern as bubbly flow, churn turbulent flow and wispy annular flow. Based on the experiences gained from previous experimental series, continuous high quality and consistency of the data have been basic requirements for these tests. In contrast to previous test series using the so-called variable gas injection of the TOPFLOW facility, the measurements were now accomplished in such a way that they reflect the evolution of the two-phase flow along the pipe under constant conditions for the gas injection. For the experiments with variable gas injection, the measurement plane is located always at the upper end of the pipe while gas is injected via orifices in the tube wall in different distances of this measurement plane. A disadvantage of the previous experiments, described in detail by Prasser et al. (2007a,b), was that the pressure at the individual positions of the gas injection varied due to the hydrostatic pressure, because the pressure was almost constant at the measurement plane.

CFD simulations for the evolution of poly-disperse bubbly flows have particularly shown that the models of bubbly coalescence and fragmentation must be further optimised (Lucas et al. 2007). At relatively small void fractions, the pressure effect on the increase in bubble size can have a larger influence on the evolution of the bubble size distribution than coalescence and fragmentation. Prasser et al. 2007b discuss which essential influence the bubble expansion may have on the bubble size distribution basing on experimental and numerical results.

Therefore, in the new series the pressure was kept constant at the respective gas injection. The measurement data represent the evolution of the flow along the pipe, as it would be observed for an injection at a constant height position with an associated shift of the measurement plane. A further disadvantage of the previous measurements was the non-constant water temperature, which varied between 20 °C and 37 °C during the measurement series. Unlike the previous series, all measurements were now performed at a nearly constant temperature of T = 30 °C. The deviations were smaller than 1 K. This is important because the coalescence rate and break-up frequency sensitively depend on the temperature caused by the effect of the surface tension. In addition, the number of the measured combinations of air and water volume flow rates was clearly increased in comparison to former measurements.

Extensive cross-checks of the plausibility of the data against each other were done. This concerns the continuous development of time averaged profiles and the bubble size distribution with increasing height scale L/D as well as the comparison of the gas volume flow obtained from measurement data with the setting data. This enables a global error assessment and shows the dependence of the precision of the measurements on the respective flow conditions. The time and cross section averaged gas volume fraction values are compared to those obtained from drift models considering profiles effects and effects of varying bubble rise velocities with varying bubble sizes.

The experiments, measuring technique, data evaluation procedures, error assessment and experimental results are described in detail in an experiment report by Beyer et al. (2008). The database is unique regarding their detailed information on important two-phase flow parameter. Since a large number of measuring points are in the region of bubbly flow it is especially, but not only, suitable for model development and validation for poly-dispersed flows. The clear trends in the evolution of the flow with increasing L/D qualifies the data e.g. for the development and validation of models for bubble coalescence and break-up. It is proposed to use the database as a benchmark for modelling poly-dispersed flows.

2. EXPERIMENTAL SETUP

2.1 TOPFLOW-Test section “Variable Gas Injection”

The measurements were carried out at the **T**ransient tw**O P**hase **FLOW** test facility (TOPFLOW) of the Institute of Safety Research at the Forschungszentrum Dresden-Rossendorf. The facility is described in detail by Beyer et al. 2004 and Prasser et al. (2006). One of the installed test section is the so-called variable gas injection (see Fig. 1), which consists of a vertical steel pipe with an inner diameter of 195.3 mm and a length of about 8 m. It is equipped with six gas injection units which allow to inject air or steam via orifices in the pipe wall. They are arranged almost logarithmically over the pipe length since the flow structure varies quite fast close to the gas injection mainly caused by the radial redistribution of the gas. Bubble coalescence and breakup which considerably determine the evolution of the flow for larger distances from the gas injection allow larger distances between the single measuring positions. Each gas injection module (Fig. 2) consists of three chambers. This gas injection via wall orifices offers the advantage that the two-phase flow can rise smoothly to the measurement plane, without being influenced by the feeder within the tube in other height positions. Two of the three chambers (the uppermost and the

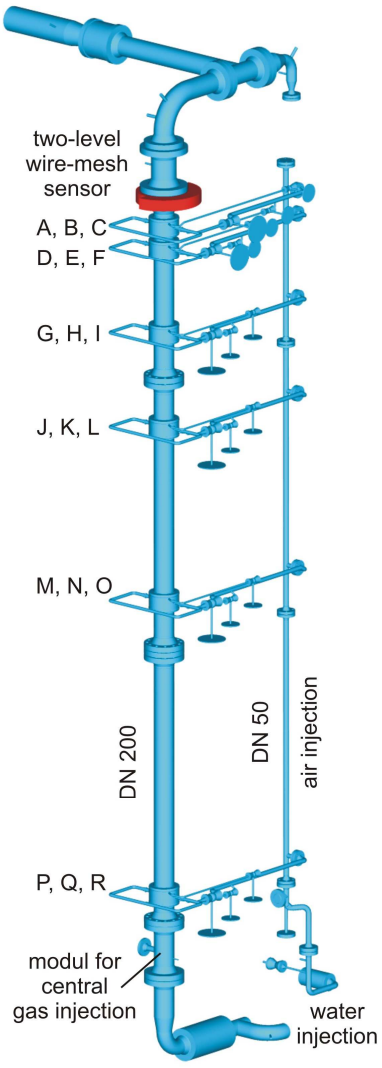

Fig. 1 Scheme of the vertical test section of the TOPFLOW facility with variable gas injection system (DN 200)

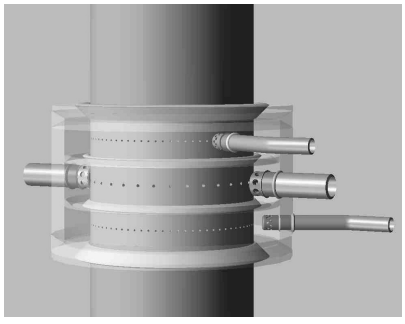

Fig. 2. Injection module of the variable gas injection

lowest) have 72 x 1 mm orifices. The middle chamber has 32 x 4 mm orifices, which is used to vary the initial bubble size distribution. For rotation–symmetric gas injection, all orifices per chambers are equally distributed over the circumference of the pipe. The injection chambers itself were designed to guarantee an equal gas feeding by all the orifices. From the measured gas volume faction distribution over the pipe cross section for the smallest distance (level A for 1mm and level B for 4 mm injection) the symmetrical distribution of the gas was confirmed.
The chambers can be operated separately and are connected with a gas injection pipe and the compressed air system (Fig. 1). The supply of the liquid phase is done from the bottom of the test section by means of an isolating valve and a 90° bend. During the experiments, a module for central gas injection has been mounted at the lower end of the test section. However, it was not employed in this test series. As a result of the large distance to the measurement plane, the influence of this component on the measured flow properties can be neglected.

The measurement plane was always situated at the upper end of the test section (Fig. 1). A wire-mesh sensor with two measuring planes was used. Tab. 1 lists the vertical distances between the individual gas injections and the first measurement plane of the wire-mesh sensor located in direction of flow.

Table 1: Denotation and positions of the gas injection chambers

Injection device	Denota-tion	Diameter of the inlet orifice [mm]	Injection length [mm]	L/D ratio
1	A	1 mm	221	1.1
1	B	4 mm	278	1.4
1	C	1 mm	335	1.7
2	D	1 mm	494	2.5
2	E	4 mm	551	2.8
2	F	1 mm	608	3.1
3	G	1 mm	1438	7.4
3	H	4 mm	1495	7.7
3	I	1 mm	1552	7.9
4	J	1 mm	2481	12.7
4	K	4 mm	2538	13.0
4	L	1 mm	2595	13.3
5	M	1 mm	4417	22.6
5	N	4 mm	4474	22.9
5	O	1 mm	4531	23.2
6	P	1 mm	7688	39.4
6	Q	4 mm	7745	39.7
6	R	1 mm	7802	39.9

2.2 Wire-mesh sensor

Numerous publications were published in the past on the wire-mesh sensor technology (e.g. Prasser et al., 1998, 2001) and on experiments using the wire-mesh sensor (e.g. Prasser et al. 2002, 2007b, Lucas et al. 2005, 2007). One measuring plane of the sensor consists of two grids of parallel wires, which span over the measurement cross-section. The wires of both planes cross under an angle of 90°, but do not touch. Instead there is a vertical distance between the wires at the crossing points. At these points the conductivity is measured. According to the different conductivity of air and water the phase present in the moment of the measurement at the crossing point can be determined. Many different types of wire-mesh sensors including such for an operational pressure up to 7 MPa and temperatures up to 290 °C were built and successfully used during the last 15 years. Also recent developments which allow measuring the capacity extent the field of applications to non-conducting fluids like oil-nitogen flows.

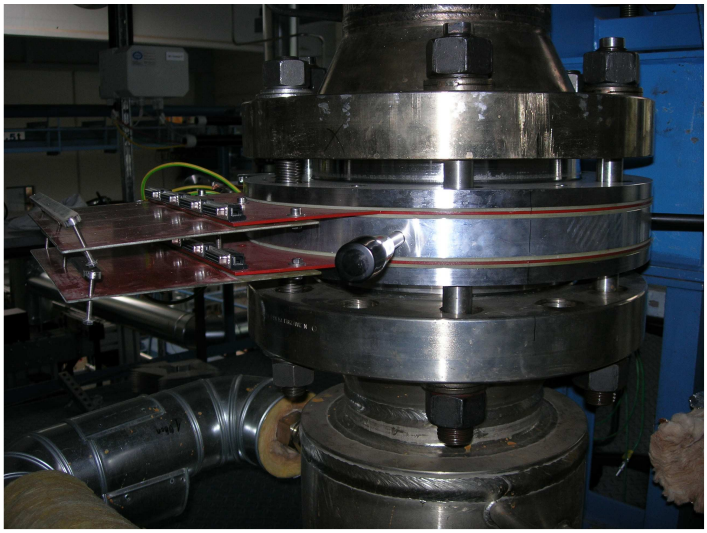

Fig. 3 The installed wire-mesh sensor with two measuring planes

In the present case, a low temperature wire-mesh sensor with two measuring planes was employed. Each plane is composed of 64 x 64 wires. It consists of two printed circuit boards (material thickness: 2.5 mm). Both of them are equipped with pre-stressed wire electrodes being soldered at a 90° angle to each other on the upper and lower surface. The wires have a lateral distance of 3 mm. In order to make the mechanical sealing of the sensor possible, the wire electrodes with a diameter of 0.125 mm were mounted in approx. 0.3 mm deeply in-milled slots on the printed circuit board. As a result of this construction form, the distance between the two grid levels arises to approx. 2 mm.

The prepared printed circuit boards are installed between two flanges and the intermediate ring (see Fig. 3). The distance of 40.5 mm between both printed circuit boards, and thus between the measurement planes results from the thickness of the intermediate ring, as well as from the pressed silicone seals. In order to reduce the weight of the sensor, the intermediate ring is partially made of aluminium. Four plastic spacer rings are used in the sensor, in order to limit the contact pressure on the silicone sealing rings and, in the case of a repeated assembling, to ensure a reproducible distance of the planes of measurement.

Measurements were done with a frequency of 2500 frames per second, i.e. 2500 pictures of the instantaneous gas distribution in the pipe cross section are obtained. The measuring time was 10 s for each single measurement, i.e. the result of one measurement is a three-dimensional matrix of 64*64*25.000 values of the instantaneous local conductivity. By a calibration procedure described below a matrix of the instantaneous local volume void fraction with the same dimensions is calculated.

2.3 Boundary conditions and measuring matrix

Special attention was paid to the pressure and temperature boundary conditions during these experiments. As stated above the pressure was kept constant at 0.25 MPa (a) at the location of the activated gas injection to represent the situation of an evolutional flow by using the different gas injections. Since a

pressure measurement is done only close to the position of the wire-mesh sensor the set pressure at this location has to be determined. This was done considering the hydrostatic pressure and the pressure drop due to friction. The gas volume fraction which is needed for this calculation was determined from the set values of the air and water superficial velocities and the assumption of a constant drift velocity of 0.25 m/s. The detailed procedure as well as an estimation of errors caused by this method can be found in the experiment report by Beyer et al. (2008).

A special operational procedure was used to keep the water temperature constant at 30 °C with a maximal deviation of 1 K. Special flow meters were used to minimize the error of the flow rates. Details on the test procedure, calibration values and errors of the operational instrumentation can also be found in Beyer et al. (2008).

Tab. 2 shows the measuring matrix, i.e. the combinations of air and water superficial velocities measured. Two test series were done with constant liquid superficial velocities of 0.405 m/s and 1.017 m/s and increasing gas superficial velocities, respectively. In two other series the gas superficial velocities were kept constant (0.0096 m/s and 0.219 m/s) and the liquid superficial velocity was varied. The colours in this table show the observed flow patterns. They were determined according to the sphere equivalent diameter of the largest gas structures observed in the flow ($d_{b,max}$ < 50 mm: bubbly flow, 50 mm < $d_{b,max}$ < 500 mm: churn turbulent flow, $d_{b,max}$ < 500 mm: annular flow).

Table 2: Test matrix: measurements were done for the coloured points. The colours mark the observed flow pattern. Yellow: bubbly flow for all L/D, green: transition from bubbly to churn turbulent flow with increasing L/D, blue: churn turbulent, red: annular flow for all L/D

Superficial water velocity J_L [m/s]	**Superficial gas velocity J_G [m/s] (at 0.25 MPa (absolute))**																
	0.0025	0.004	0.0062	0.0096	0.0151	0.0235	0.0368	0.0574	0.0898	0.14	0.219	0.342	0.534	0.835	1.305	2.038	3.185
1.611	009	020	031	042	053	064	075	086	097	108	119	130	141	152	163	174	185
1.017	008	019	030	041	052	063	074	085	096	107	118	129	140	151	162	173	184
0.641	007	018	029	040	051	062	073	084	095	106	117	128	139	150	161	172	183
0.405	006	017	028	039	050	061	072	083	094	105	116	127	138	149	160	171	182
0.255	005	016	027	038	049	060	071	082	093	104	115	126	137	148	159	170	181
0.161	004	015	026	037	048	059	070	081	092	103	114	125	136	147	158	169	180
0.102	003	014	025	036	047	058	069	080	091	102	113	124	135	146	157	168	179
0.0641	002	013	024	035	046	057	068	079	090	101	112	123	134	145	156	167	178
0.0405	001	012	023	034	045	056	067	078	089	100	111	122	133	144	155	166	177

For investigations on the evolution of the flow along the pipe, all levels (A-R) shown in Tab. 1 and Fig. 1, were measured for any points smaller than 149. The maximum possible gas flow rate, which can be injected through the injection chambers with a diameter of 1 mm, is limited. For this reason for the points 149, 151, 160 and 162 both injection chambers with 1 mm orifices were operated parallel. For the measurement points 171, 173, 182, 184 only the 4 mm injections were used.

3. DATA OBTAINED

From the raw data, i.e. the 64*64*25.000 matrix of voltage signals representing the instantaneous local conductivity a matrix with the same dimensions containing the according void fraction values are obtained by a calibration procedure. The conductivity of the gas is negligibly small. Two calibration methods are applied – the so-called histogram calibration and the use of calibration files. The latter ones are obtained by measurements for pure water flow from which the pure water signal level is determined. The disadvantage of this method is that the conductivity of the water may slightly change with time by different causes. For this reason the histogram calibration is preferred which obtains the pure water signal level directly from the measured data. A histogram of the measured voltage values is generated for each crossing point of the wire-mesh sensor and each single measurement. Usually two peaks are observed in these histograms – one (close to zero) representing the pure gas the other the pure liquid value. The disadvantage of this method is that it fails for flows with very high gas leads where only few values for pure water are available. In a mixed approach the histogram method is used first. The obtained radial profiles for the pure water calibration values are evaluated afterwards. In case they show inconsistencies in the pipe centre (where the void fraction is largest) calibration files are used. Once the calibration values are determined for each matrix point the void fraction values are calculated assuming a linear dependence between voltage values and gas volume fraction.

The 64*64*25.000 matrix of void fraction values now can be used to obtain relevant data by averaging procedures. By averaging over the pipe cross section **time series of the void fraction** are obtained. The according averaging procedure considers the smaller measuring volumes in the region of the pipe wall by individual weight coefficients for the single meshes. Most important is the time averaging, which e.g. leads to time averaged **two-dimensional gas volume fraction distributions in the pipe cross section**. Due to the radial symmetry of the data the statistical error can be further lowered by an azimuthally averaging. To do this the cross section is sub-divided into 80 ring-shaped domains with equal radial width. The contribution of each mesh is calculated by weight coefficients obtained from a geometrical assignment of the fractions of a mesh belonging to these rings. In the results **radial gas volume fraction profiles** are obtained. An example of such profiles is shown in Fig. 4. At small L/D the gas is still concentrated close to the wall since it was injected from the wall. Due to bubble forces (especially due to lift force which has a negative lift force coefficient for the large bubbles) the profiles changes to a centre peak profile with increasing L/D.

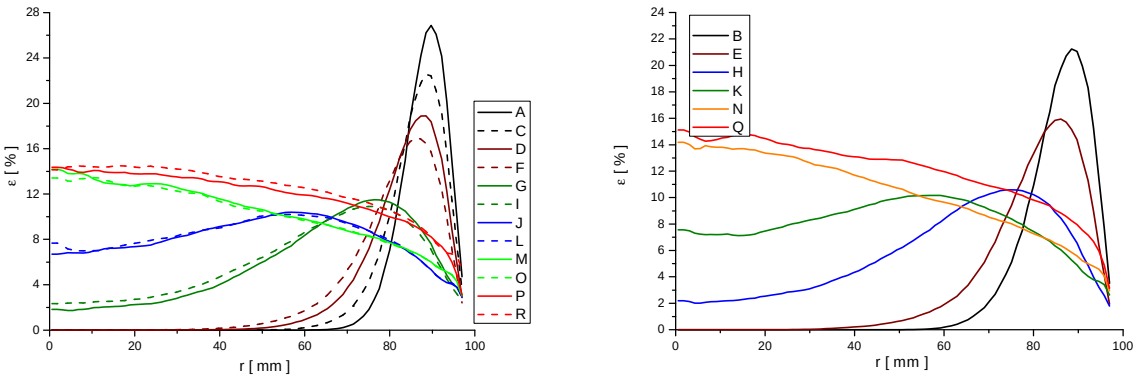

Fig. 4 Examples for evolution of the radial gas volume fraction profiles with increasing distance between gas injection and measuring plane. J_L = 1.017 m/s, J_G = 0.0898 m/s, left: injection via 1 mm orifices, right: injection via 4 mm orifices, denotation of the injection chambers used and assigned L/D see Tab. 2.

As mentioned above a sensor with two measuring planes was used. This allows to cross-correlate the gas volume fraction values of the two-planes for all mesh point which are located above each other. From the maxima of the cross-correlation functions the typical time shift of the local void fraction fluctuations can be determined. Since the distance between the measuring planes is known the local time averaged gas velocity can be calculated. The point-to-point **two-dimensional gas velocity distributions in the pipe cross section** are obtained in the results of this procedure. Again an azimuthally averaging is applied to obtain the **radial profiles of the gas velocity**. An example for such radial profiles of the gas velocity is given in Fig. 5. In spite of the averaging some single outliers were observed in the radial profiles. They were identified manually and replaced by an averaged value obtained from the two neighbouring radial rings. The corrections done are documented in the experimental report by Beyer et al. (2008).

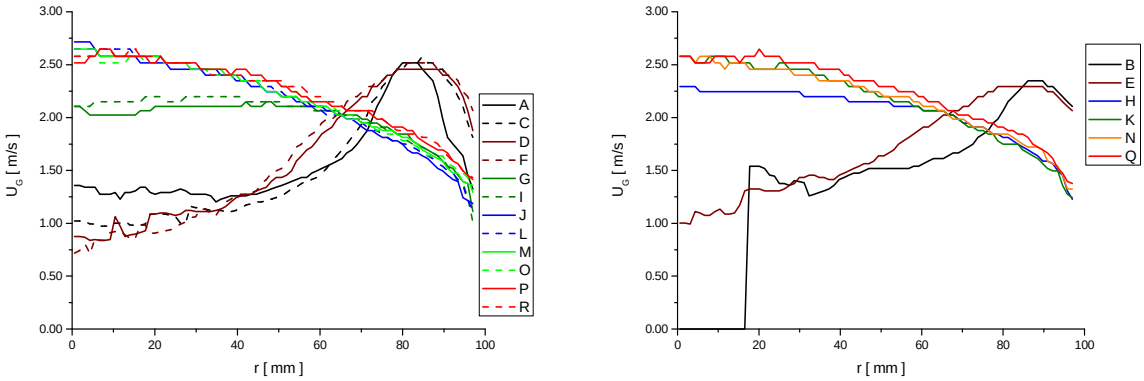

Fig. 5 Examples for evolution of the radial gas velocity profiles with increasing distance between gas injection and measuring plane. J_L = 1.017 m/s, J_G = 0.534 m/s, left: injection via 1 mm orifices, right: injection via 4 mm orifices, denotation of the injection chambers used and assigned L/D see Tab. 2.

The next step of the data evaluation procedure is the identification of single bubbles. Thereby, a bubble is defined as a region of connected gas-containing elements in void fraction matrix which is completely surrounded by elements containing the liquid phase. A complex procedure, described by Prasser et al. (2001), applies filling and agglomeration algorithms combined with sophisticated stop criteria to avoid artificial combinations as well as artificial fragmentation of bubbles. In the result to each element which belongs to one bubble, the same identification number is assigned. Different bubbles receive different identification numbers. These numbers are stored in the elements of a second array. This array has the same dimension as the void fraction array. Combining the information from the void faction and bubble number arrays together with the radial profiles of the gas velocity characteristic **data of the single bubbles as bubble volume, sphere equivalent bubble diameter, maximum circle equivalent bubble diameter in the horizontal plane, coordinates of the bubble centre of mass, moments characterizing asymmetries** and others are obtained. Basing on these data **cross section and time averaged bubble size distributions** (see Fig. 6) and **radial gas volume fraction profiles decomposed according to the bubble size** are calculated. The bubble size distributions are defined volume fraction related, i.e. they present the volume fraction per bubble diameter (equivalent diameter of a sphere with the measured bubble volume V_b).

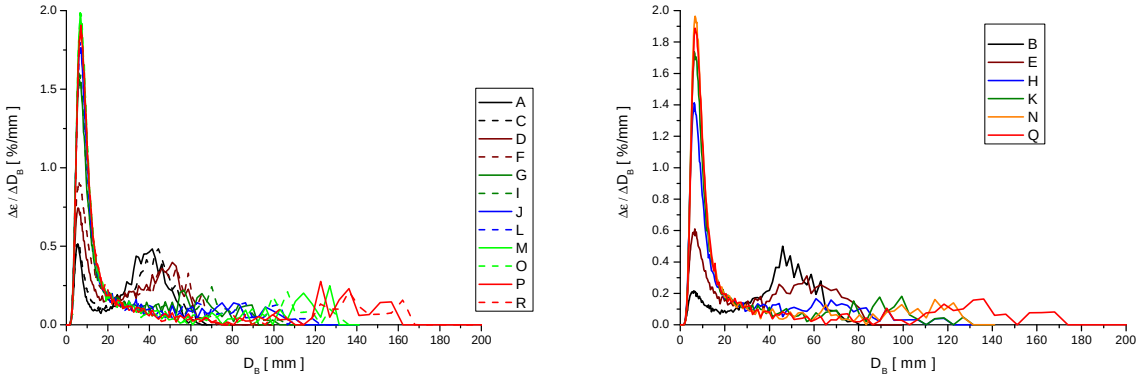

Fig. 6 Examples for evolution of bubble size distributions with increasing distance between gas injection and measuring plane. J_L = 0.641 m/s, J_G = 0.219 m/s, left: injection via 1 mm orifices, right: injection via 4 mm orifices, denotation of the injection chambers used and assigned L/D see Tab. 2.

4. CHECKS OF ACCURACY

4.1 Errors of boundary conditions and wire-mesh sensor measurements

All the standard instrumentation of the TOPFLOW facility as mass flow controllers or pressure transducer used are calibrated and have maximum errors in the order of 1%. Calibration protocols as well as the data regarding the accuracy for each single instrumentation is given in the experiment report by Beyer et al. (2008).

To set a constant pressure at the gas injection (0.25 MPa (a)), the two-phase pressure drop in the test section was calculated to define the pressure boundary condition at the position of the pressure measurement (see section 2.3). A constant velocity of 0.25 m/s was assumed for the calculation of the void fraction which influences the pressure drop. After completion of the experiments a “weighted drift velocity” was obtained (see section 4.4) for each single measurement. This information was used to re-check the calculated set pressure values and to compare the results with the ones obtained for the assumed constant drift velocity. For most of the measurements the errors are clearly less than 1%, only in cases with high gas volume fractions (measuring matrix points 111-116, 127, 138, 149, 151, 160, 162, 171, 173, 182, 184, see Tab. 2) some larger errors up to 3.5 % occur.

Errors of the wire-mesh sensor measurements for the gas fraction and bubble size are mainly caused by the lateral pitch of the wires which is 3 x 3 mm and the distance of the wire planes which is 2 mm. Comparative measurements between the wire-mesh sensor and other research methods supplied information on the accuracy of the measurement technique and the evaluation algorithms for the experimental determination of these flow parameters. Gamma radiography of an air/water flow for varying superficial velocities of both media resulting in a gas volume fraction between 0 and 100 % showed that the deviations between wire-mesh sensor and gamma measurement are limited to ± 5 % (Prasser 2000). The radiography of a steam/water flow at atmospheric pressure confirmed this statement (Manera et al. 2001). It has to be considered that the reference procedure has measurement errors, too. Comparative measurements between wire-mesh sensor and an X-ray tomography, which is a more exact reference procedure, were also done for air/water flow. As a result of this investigation it was found, that the accuracy of the gas volume fraction averaged over the flow cross-section depends on the two-phase

flow regime. Differences in the absolute void fraction were determined (Prasser et al. 2005) for a bubbly flow in the range of ± 1 % and at slug flow, a systematic underestimation of approx. - 4 %.

Comparative measurements with a high-speed camera are available to estimate the measurement error for the determination of the volume equivalent bubble diameter. The investigations were performed in a transparent flow channel DN100 where air/water flows with different bubble sizes. Scholz 2000 demonstrated that only bubbles with a diameter larger 1.6 mm can be recorded due to the limited spatial resolution in case of a wire-mesh sensor with a pitch of the wires of 3 x 3 mm. In addition, the comparisons between the data of the wire-mesh sensor and the high-speed camera showed that the volume equivalent diameter is measured at superficial water velocities of > 0.2 m/s with an accuracy of ± 20 %. At smaller water velocities, overestimations up to + 50 % were observed. Note that the dispersion of the determined bubble sizes under constant flow conditions is significantly larger for the high-speed camera measurement than for the wire-mesh sensor. For this reason, it is assumed that the indicated deviations between both procedures mainly results from the inaccuracy of the optical method.

The distance between the two measuring planes of the wire-mesh sensor used (40.5 mm) causes a discretization error for the gas velocity determined by the cross-correlation measurement of about 4% for the largest gas velocity (point 184) but is lower than 1% for all points of the measuring matrix ≤ 118.

4.2 Consistency of the data

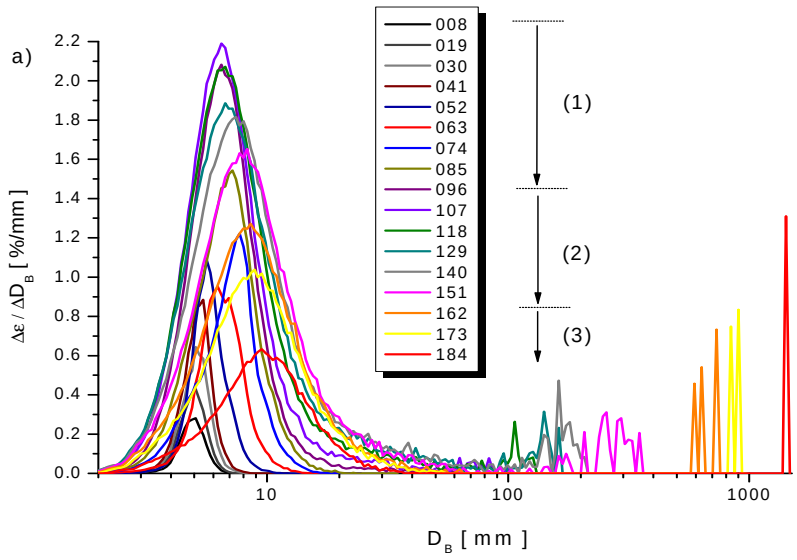

Fig. 7 Bubble size distributions in dependence on the gas superficial velocity (values see Tab. 2) and constant liquid superficial velocity J_L = 1.017 m/s, gas injection via 1 mm orifices, L/D = 39.9, (1) bubbly flow, (2) churn turbulent flow, (3) transition to wispy annular flow with some large structures

The radial profiles of the gas volume fraction and the gas velocity as well as the cross-section averaged bubble size distributions are plotted in the experimental report by Beyer et al. (2008) for all measuring points. Figs. 4 – 6 show some examples of these plots. A clear trend of the data with increasing L/D can be seen at these figures. There are no jumps in the evolution of the curves. The plausibility and the evolution with increasing L/D were checked for all the measurements. In the result it was found, that the data fit very well to each other. For all data clear trends are observed and show a logical order. This is especially important for the use of the data to develop and validate models for bubble forces and bubble coalescence and fragmentation.

A cross-check of the results of the different points of the measuring matrix was also done. Fig. 7 shows as an example the measured bubble size distribu-tions for largest L/D in case of the 1 mm injection for

varying gas superficial velocity and constant liquid superficial velocity. Also for these checks the clear and plausible trends of the data can be confirmed. The largest bubble size observed in a measurement was used as a criterion to define the flow pattern, which is also shown at Fig 7.

4.3 Reconstructed gas volume flow rates

From the measured radial profiles of the void fraction and the velocity of the gas phase, the superficial gas velocity at the sensor can be calculated by integrating the product of both profiles over the pipe radius. Dependent on the test section height, the superficial gas velocity at the wire-mesh sensor can be obtained from the set values at the location of the active gas injection (i.e. at 0.25 MPa (a), see Tab. 2) by considering the Boyle-Mariotte`s law. Fig. 8 shows the comparison of the gas superficial velocities obtained from the measurement compared with the values obtained from the set values. In general there is a good agreement, but some systematic overestimation of the gas volume flow rate can be observed for low gas flow rates, independent on the size of the injection orifices used. It was found, that the relative overestimation for cases with small gas volume fractions, i.e. for cases with bubbly flow is at about 20%. This is not in conflict with the above mentioned error estimations since they were related to absolute errors.

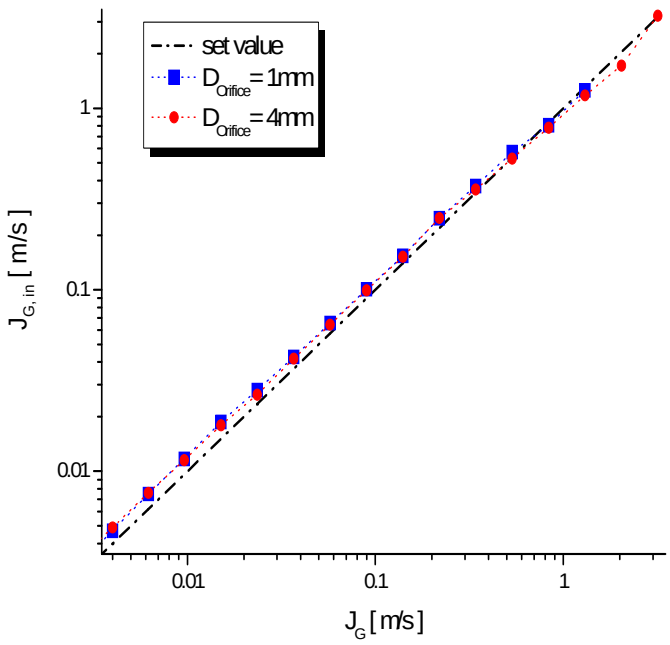

Fig. 8 Comparison of the superficial gas velocity J_G calculated from experimental data with the set values for maximum L/D for J_L = 1.017 m/s with different gas injection orifices

Note that the deviations from the set value result from both the gas fraction and the velocity measurement. The reasons for the overestimation are presently under investigation. It can be assumed, that it is connected with the wire-mesh signals obtained in the case that the interface is between both layers of wires, i.e. also the vertical distance between the wires may play a role. A deceleration of the bubbles due to the contact with the wires was observed for low liquid velocities but should not be the reason for the deviations shown in Fig. 8 for J_L = 1.017 m/s. Nevertheless this effect is important in case of liquid superficial velocities below 0.4 m/s (points of the measuring matrix 034-038 and 111-115. For these points larger overestimations are observed. The results of this check are documented in detail in the experimental report by Beyer et al. (2008).

4.4 Plausibility of integral void fraction values

The aforementioned comparison of the gas superficial velocities obtained from the measurements with the set values always checks the gas volume fraction together with the gas velocity. An inaccuracy also arises from the fact, that only one velocity value is used for a given radial position of a bubble, i.e. the dependency of the bubble velocity on their size is neglected. In principle, this could be considered during the data evaluation, the statistical uncertainty, however, would be too high. For this reason here a mixed approach using correlations and measured radial profiles and bubble size distributions is applied to check the plausibility of the measured values of the time and cross-section averaged gas volume fraction.

The gas volume fraction can be calculated from the superficial velocities of both phases J_L and J_G and the drift velocity U_D according to:

$$\varepsilon = \frac{J_G}{J_G + J_L + U_D}. \tag{1}$$

While J_L is the set value J_G has to be calculated from the set value at injection using the Boyle-Mariotte law due to the lower pressure at the measuring plane. A raw estimation of the void fraction can be done assuming a constant value of the drift velocity of 0.235 m/s which is a good representation for bubbles in the range of 4 to 10 mm equivalent bubble diameter. Examples for the results are shown in Fig. 9 (green curves). The trend of the void fraction with increasing L/D can also be tested by adopting a value for the drift velocity obtained from the largest L/D measured. Such curves are also shown in Fig. 9 (red). The general trend resulting from the decreasing pressure with increasing L/D is reflected by these curves, but clear deviations occur close to the injection.

The drift velocity considering profile effects as well as the size dependent local bubble velocity can be calculated according to:

$$U_D = (C_0 - 1)J + U_{GJ}, \tag{2}$$

with the profile factor C_0 and the averaged local drift velocity U_{GJ}:

$$C_0 = \frac{2}{R^2 \langle \varepsilon \rangle \langle j \rangle} \int_0^R j(r)\varepsilon(r) r dr, \quad U_{GJ} = \frac{2}{R^2 \langle \varepsilon \rangle} \int_0^R \sum_i (u_{D,i}\varepsilon_i(r)) r dr. \tag{3}$$

$\langle X \rangle$ stands for the cross section averaged values, j is the local superficial velocity, $\varepsilon_i(r)$ the gas volume fraction profile decomposed according to the bubble size class i, u_{Di} the local drift velocity of bubbles of class i and R is the pipe radius. The local drift velocity is calculated from a correlation for the terminal velocity of a bubble of size $d_{b,i}$ and a swarm correction. The according correlations and the complete procedure are described by Beyer et al. (2008). It should be considered, that for the calculation measured radial profiles are used, but they are normalized by their integral value what limits the influence of the measurement on the values obtained for the drift velocity. Combining eqs. (1)-(3) slopes of the gas volume fraction in dependency on L/D can be calculated. Examples are shown in Fig. 9, blue curves. They reflect the trends of the measured values also in the region close to the injection. Nevertheless there is a systematic shift of the curves. This is an indication for a slight overestimation of the measured gas volume fraction. The different behaviour of the curves close to the injection results from profile effects. In case of low void fraction the profile of the liquid velocity (Fig. 9, left) remains nearly unchanged, i.e. the velocity of the gas injected from the wall is low. In case of larger void fractions (Fig. 9, right) the liquid is accelerated in the wall region by the injected bubbles and secondary flows occur (see also Fig. 5, right). This causes higher gas velocities and thus lower void fraction values in the vicinity of the injection.

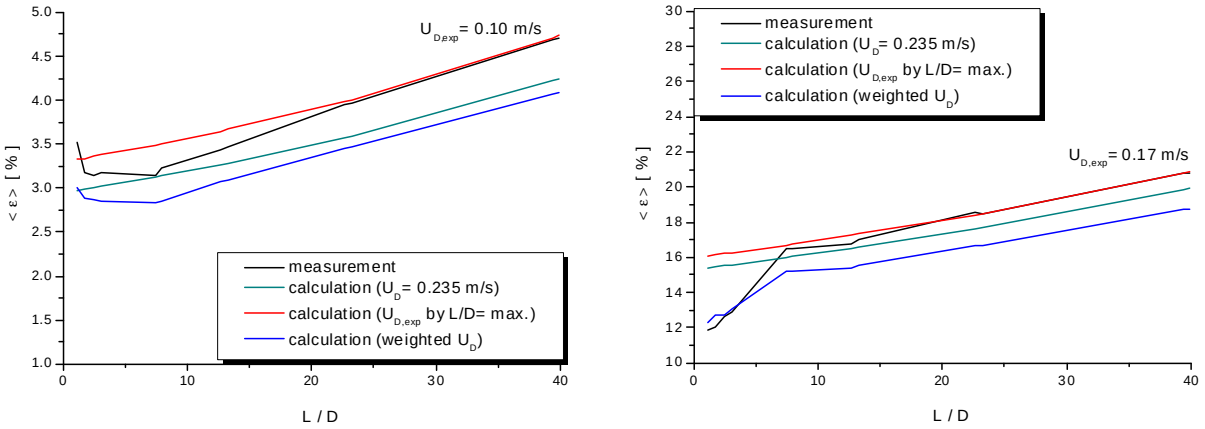

Fig. 9 Examples for the dependency of the gas volume fraction on the relative test section height L/D. The measured values are compared with values resulting from the assumption of a drift velocity equal to 0.235 m/s, a drift velocity adapted to the measures void fraction value for largest L/D and resulting from eqs. (1)-(3). J_L = 1.017 m/s, left J_G = 0.0368 m/s, right: J_G = 0.219 m/s, injection via 1 mm orifices.

5. SUMMARY

A detailed database for air-water flow in a vertical pipe with an inner diameter of 195.3 mm for a wide range of flow rates was established. It contains CFD-grade data for the evolution of the flow along the pipe including radial profiles of the void fraction and the gas velocity as well as bubble size distributions. Also double-differential void fraction data regarding radial position and bubble size are available. Extensive checks were done regarding the data quality. It was found, that the consistency of the data to each other is excellent, while a slight overestimation of the measured integral void fraction has to be considered. Nevertheless the data in their detailedness are unique world-wide and probably have the best quality. A detailed documentation of the experiments and the quality checks is given by Beyer et al. (2008). It is proposed to establish the database as international benchmark for the simulation of poly-dispersed bubbly flows.

NOMENCLATURE

C_0	[-]	Profile factor
D	[m]	Pipe diameter
L	[m]	Distance between gas injection and measuring plane
J	[m/s]	Superficial velocity
j	[m/s]	Local volume flow rate
U	[m/s]	Velocity
R	[m]	Pipe radius
r	[m]	Radial coordinate
ε	[-]	Gas volume faction

Indizes

D	Drift
G	Gas
i	Bubble class
L	Liquid

ACKNOLEDGEMENTS

This work is carried out in the frame of a current research project funded by the German Federal Ministry of Economics and Labour, project number 150 1329. The authors like to thank all members of the TOPFLOW team who contributed to the successful performance of these experiments.

REFERENCES

Beyer, M., Carl, H., Schütz, P., Pietruske, H., Lenk, S., "Betriebshandbuch für die Mehrzweck-Thermohydraulikversuchsanlage TOPFLOW" Report *FZR-405*, (2004).
Beyer, M., Lucas, D., Kussin, J., Schütz, P., "Air-water experiments in a vertical DN200-pipe", FZD-Report, (2008).
Lucas , D. Krepper, E., Prasser, H.-M., "Development of co-current air–water flow in a vertical pipe", *International Journal of Multiphase Flow*, 31, 1304–1328, (2005).
Lucas, D., Krepper, E., Prasser, H.-M., "Modelling of the evolution of bubbly flow along a large vertical pipe", *Nuclear Technology*, 158, 291-303, (2007).
Manera, A., Prasser, H.-M., Van der Hagen, T. H. J. J., Mudde, R. F., de Kruijf, J. M., "A comparison of void-fraction measurements during flashing-induced instabilities obtained with a wire-mesh sensor and a gamma-transmission set-up", *4th Int. Conf. on Multiphase Flow*, New Orleans, USA, paper: 436 (2001).
Prasser, H.-M., Böttger, A., Zschau, J., "A new electrode-mesh tomograph for gas/liquid flows", *Flow Measurement and Instrumentation* 9, 111 – 119, (1998).
Prasser, H.-M., "High-speed measurement of the void fraction distribution in ducts by wire-mesh sensors", *International Meeting on Reactor Noise*, Athen, (2000).
Prasser, H.-M., Scholz, D., Zippe, C., "Bubble size measurement using wire-mesh sensors", *Flow Measurement and Instrumentation*, 12, 299-312 (2001).
Prasser, H.-M., Krepper, E., Lucas, D., "Evolution of the two-phase flow in a vertical tube - decomposition of gas fraction profiles according to bubble size classes using wire-mesh sensors", *International Journal of Thermal Sciences*, 41, 17-28, (2002).
Prasser, H.-M., Misawa, M., Tiseanu, I., "Comparison between Wire-mesh sensor and ultra-fast X-ray tomograph for an air/water flow in a vertical pipe", *Flow Measurement and Instrumentation*, 16, 73-83 (2005).
Prasser H.-M., Beyer, M., Carl, H., Manera, A., Pietruske, H., Schütz, P., Weiß, F.-P., " The multipurpose thermal-hydraulic test facility TOPFLOW: an overview on experimental capabilities, instrumentation and results", *Kerntechnik*, 71, 163-173, (2006).
Prasser, H.-M., Beyer, M., Carl, H., Manera, A., Pietruske, H., Schütz, P., "Experiments on upwards gas/liquid flow in vertical pipes", Report *FZD-482*, (2007a).
Prasser, H.-M., Beyer, M., Carl, H., Gregor, S., Lucas, D., Pietruske, H., Schütz, P., Weiss, F.-P., "Evolution of the structure of a gas–liquid two-phase flow in a large vertical pipe", *Nuclear Engineering and Design* 237, 1848–1861 (2007b).
Scholz, D., "Bewertung der Genauigkeit eines Gittersensors zur Visualisierung einer Zweiphasen-strömung durch Vergleich mit optischen Hochgeschwindigkeitsaufnahmen", *Report FZR-300* (2000).